Two-Dimensional Structure of Disulfides and Thiols on Gold(111)

Gabriele Nelles,[†] Holger Schönherr,[‡,§] Manfred Jaschke,[†] Heiko Wolf,[‡] Matthias Schaub,[∥] Jörg Küther,[⊥] Wolfgang Tremel,[⊥] Ernst Bamberg,[†] Helmut Ringsdorf,[‡] and Hans-Jürgen Butt*[,#]

Max-Planck-Institut für Biophysik, Kennedyallee 70, D-60596 Frankfurt/Main, Germany, Institut für Organische Chemie, Institut für Anorganische und Analytische Chemie, and Institut für Physikalische Chemie, J. Gutenberg-Universität Mainz, D-55099 Mainz, Germany, and Department of Chemistry, Massachusetts Institute of Technology, Cambridge, Massachusetts 02139

Received August 28, 1997. In Final Form: November 18, 1997

In order to find factors which determine the two-dimensional structure of self-assembled monolayers (SAMs), several classes of thiols and disulfides on gold (111) have been investigated by atomic force microscopy (AFM). SAMs were formed from a series of symmetrical and asymmetrical diethylalkanoate disulfides, ω-hydroxy- and ω-carboxyalkanethiols, diacetylene disulfides, and different anthracene terminated thiols and disulfides. In all the cases, two-dimensional crystalline structures could be resolved; even for an asymmetrical diethylalkanoate disulfide that had a chain length difference of five methylene units. The lattices were analyzed quantitatively. Two distinctly different types of crystalline structures were observed, namely, a hexagonal and a centered rectangular lattice. For the diethylalkanoate disulfides with short alkyl chains ($n \leq 10$) both structural phases were observed, domains with a hexagonal lattice existing simultaneously with centered rectangular domains. The length of the alkyl chain determined the probability of finding disulfides in the hexagonal structure. This dependence on the shape of the molecules as well as the clear contrast of SAMs of asymmetric disulfides suggest that the AFM tip penetrates into the SAMs and probes, at least partially, the interior of the layers. With the atomic force microscope no difference was observed between SAMs formed from thiols and those from disulfides.

Introduction

Many thiols and disulfides form highly ordered self-assembled monolayers (SAMs) on gold surfaces.[1−7] The binding to the surface is strong, as seen from high binding energies which are of the order of 120 kJ/mol,[2,8,9] as well as the high mechanical stabilities of alkanethiol SAMs.[10−12] In addition, SAMs of thiols are stable over long periods.[5] By choosing appropriate thiols or disulfides, SAMs with different properties can be formed in a well-defined and predetermined way (reviewed in refs 13−17). They are therefore often used to study the process of self-assembly and, more generally, as model systems of organic surfaces and interfaces on solid substrates.

The best studied SAMs are those formed by long-chain *n*-alkanethiols or disulfides. On gold(111) and amorphous gold surfaces they form a two-dimensional hexagonal crystalline structure with a lattice constant of 5.0 Å.[12,18−24] The two-dimensional structure of other thiols and disulfides have also been determined. Examples are perfluoroalkylthiols and disulfides,[25,26] azobenzenethiols,[27,28] and several mixed alkanoate/perfluoroalkanoate disulfides.[28,29] Understanding the interrelationships between the molecular structure of a molecule and its organization

* To whom correspondence should be addressed.
[†] Max-Planck-Institut für Biophysik.
[‡] Institute für Organische Chemie, J. Gutenberg-Universität Mainz.
[§] Present address: Faculty of Chemical Technology, University of Twente, P.O. Box 217, 7500 AE Enschede, The Netherlands.
[∥] Massachusetts Institute of Technology.
[⊥] Institut für Anorganische und Analytische Chemie, J. Gutenberg-Universität Mainz.
[#] Institut für Physikalische Chemie, J. Gutenberg-Universität Mainz.

(1) Nuzzo, R. G.; Allara, D. L. *J. Am. Chem. Soc.* **1983**, *105*, 4481.
(2) Nuzzo, R. G.; Fusco, F. A.; Allara, D. L. *J. Am. Chem. Soc.* **1987**, *109*, 2358.
(3) Porter, M. D.; Bright, T. B.; Allara, D. L.; Chidsey, C. E. D. *J. Am. Chem. Soc.* **1987**, *109*, 3559.
(4) Troughton, E. B.; Bain, C. D.; Whitesides, G. M.; Nuzzo, R. G.; Allara, D. L.; Porter, M. D. *Langmuir* **1988**, *4*, 365.
(5) Bain, C. D.; Troughton, E. B.; Tao,Y. T.; Evall, J.; Whitesides, G. M.; Nuzzo, R. G. *J. Am. Chem. Soc.* **1989**, *111*, 321.
(6) Nuzzo, R. G.; Dubois, L. H.; Allara, D. L. *J. Am. Chem. Soc.* **1990**, *112*, 558.
(7) Hähner, G.; Wöll, C.; Buck, M.; Grunze, M. *Langmuir* **1993**, *9*, 1955.
(8) Nuzzo, R. G.; Zegarski, B. R.; Dubois, L. H. *J. Am. Chem. Soc.* **1987**, *109*, 733.
(9) Tupper, K. J.; Colton, R. J.; Brenner, D. W. *Langmuir* **1994**, *10*, 2041.
(10) Dürig, U.; Züger, O.; Michel, B.; Häussling, L.; Ringsdorf, H. *Phys. Rev. B* **1993**, *48*, 1711.
(11) Thomas, R. C.; Houston, J. E.; Michalske, T. A.; Crooks, R. M. *Science* **1993**, *259*, 1883.
(12) Liu, G. Y.; Salmeron, M. B. *Langmuir* **1994**, *10*, 367.
(13) Ulman, A. *Ultrathin Organic Films*; Academic Press: San Diego, 1991.
(14) Dubois, L. H.; Nuzzo, R. G. *Annu. Rev. Phys. Chem.* **1992**, *43*, 437.
(15) Xu, J.; Li, H. J. *J. Colloid Interface Sci.* **1995**, *176*, 138.
(16) Ulman, A. *Chem. Rev.* **1996**, *96*, 1533.
(17) Poirier, G. E. *Chem. Rev.* **1997**, *97*, 1117.
(18) Strong, L.; Whitesides, G. M. *Langmuir* **1988**, *4*, 546.
(19) Chidsey, C. E. D.; Liu, G. Y.; Rowntree, P.; Scoles, G. *J. Chem. Phys.* **1989**, *91*, 4421.
(20) Chidsey, C. E. D.; Loiacono, D. N. *Langmuir* **1990**, *6*, 682.
(21) Camillone, N.; Chidsey, C. E. D.; Liu, G. Y.; Putvinski, T. M.; Scoles, G. *J. Chem. Phys.* **1991**, *94*, 8493.
(22) Alves, C. A.; Smith, E. L.; Porter, M. D. *J. Am. Chem. Soc.* **1992**, *114*, 1222.
(23) Dubois, L. H.; Zegarski, B. R.; Nuzzo, R. G. *J. Chem. Phys.* **1993**, *98*, 678.
(24) Butt, H.-J.; Seifert, K.; Bamberg, E. *J. Phys. Chem.* **1993**, *97*, 7316.
(25) Alves, C. A.; Porter, M. D. *Langmuir* **1993**, *9*, 3507.
(26) Liu, G.; Fenter, P.; Chidsey, C. E. D.; Ogletree, D. F.; Eisenberger, P.; Salmeron, M. *J. Chem. Phys.* **1994**, *101*, 4301.

S0743-7463(97)00970-0 CCC: $15.00
Published on Web 01/22/1998

on surfaces is of great importance in many technical applications. The packing and orientation in a SAM affects the surface chemistry and is responsible for particular applications such as molecular recognition and sensor activity.[30] It is also important for patterning and nanolithography[31] as well as in microelectronics.[32]

In this work, the lateral, two-dimensional structure of SAMs of a series of thiols and disulfides on gold(111) was investigated by atomic force microscopy (AFM). In particular, the influence of an ester group midway in the alkyl chains on the crystallinity of the structure was examined with respect to the chain length. Furthermore the influence of the end groups on the crystallinity of the structure was investigated by choosing sterically bulky end groups. The use of asymmetrical diethylalkanoate disulfides helped in understanding the origins of the observed contrast. Several types of thiols and disulfides were investigated: Symmetrical diethylalkanoate disulfides $[H_3C(CH_2)_nCOO(CH_2)_2S]_2$ with different chain lengths (n = 6, 8, 10, 12, 15, 16), diacetylene disulfides, several anthracene terminated thiols and disulfides, asymmetrical diethylalkanoate disulfides $H_3C(CH_2)_nCOO(CH_2)_2S-S(CH_2)_2OOC(CH_2)_mCH_3$ (m = 16, n = 11...15), and ω-hydroxy- and ω-carboxyalkanethiols. After adsorption of these thiols and disulfides, the resulting two-dimensional structures of the SAMs were investigated by AFM.

Experimental Section

Materials. The synthesis and characterization of the symmetrical diethylalkanoate disulfides $[H_3C(CH_2)_nCOO(CH_2)_2S]_2$ (n = 6, 8, 10, 12, 15, 16) are described in ref 28 and of the diacetylene disulfide $[H_3C(CH_2)_{13}C{\equiv}CC{\equiv}C(CH_2)_9COO(CH_2)_2S]_2$ in ref 33. The synthesis of the anthracene derivatives $(C_{14}H_9)COO(CH_2)_{11}SH$ and $[(C_{14}H_9)COO(CH_2)_{11}S]_2$ with anthracene bound in the 2 or 9 position is described in ref 34. Finally the synthesis of the asymmetrical diethylalkanoate disulfides $(H_3C(CH_2)_nCOO(CH_2)_2S-S(CH_2)_2OOC(CH_2)_mCH_3$ (m = 16, n = 11−15)) and the ω-hydroxy- and ω-carboxyalkanethiols are described in refs 35 and 36, respectively. Some representative examples of the different types of thiols investigated are depicted in Figure 1.

Preparation of Samples. Gold(111) substrates were prepared by evaporating 100 nm gold onto freshly cleaved mica in a vacuum of roughly 10^{-6} mbar at a gold evaporation rate of 0.2 nm/s (*Baltec* MED 020). After evaporation, the mica supported gold films were placed in a homemade annealing chamber.[28] The gold samples were held in a 0.1 mbar of argon atmosphere, and their temperature was ramped up to approximately 400 °C within 1 min by means of a resistive heating plate. Subsequently the gold substrates were quenched and rinsed with methanol and immersed into a 10^{-4} or 10^{-3} M solution of the corresponding thiol or disulfide in methylene chloride or ethanol. The adsorption times were between 18 and 20 h. The quality of the gold was checked by occasionally imaging bare gold samples. Flat domains with a size of several hundred nanometers were observed. In these domains the typical hexagonal packing of gold atoms for gold(111) with a lattice constant of 2.9 Å was observed. On thiol covered samples steps with heights equal to multiples of 2.5 Å were always observed, which corresponds to a height expected for layers of gold atoms. In addition, triangular terraces were observed on some samples; this is a clear indication for gold(111).

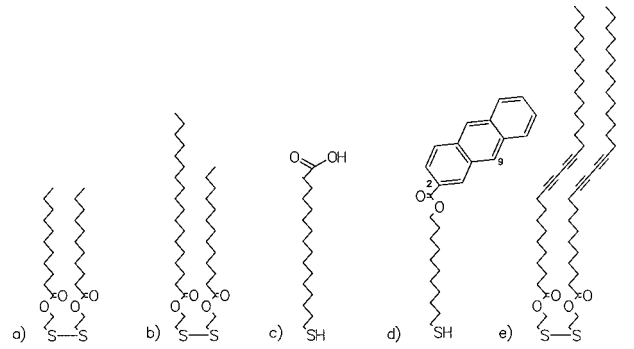

Figure 1. Examples of the different types of thiols and disulfides investigated: (a) a symmetrical disulfide bis[2-(dodecanoyloxy)ethyl] disulfide (n = 10), (b) an asymmetrical disulfide 2-(octadecanoyloxy)-2′-(tridecanoyloxy)-1,1′-diethyl disulfide (m = 16, n = 11), (c) ω-carboxyalkanethiol, (d) an anthracene terminated alkanethiol with anthracene bound at the 2 position, and (e) diacetylene disulfide.

Atomic Force Microscopy. The measurements were performed in a fluid cell of an AFM (Nanoscope III, Digital Instruments, Santa Barbara, CA). The samples were imaged in ethanol in contact mode using silicon nitride cantilevers of 100 μm length with integrated sharpened tips (spring constant, 0.09 N/m; Olympus, Tokyo, Japan). Imaging in ethanol and using relatively soft cantilevers allowed reduction of the force between tip and sample down to 0.1 nN. Typical values for the used imaging forces were between 0.2 and 3 nN. Higher forces were avoided because simulation studies suggest that at higher forces the structure of the underlying film might change locally.[37,38] However, the contrast obtained with a relatively high force of 1−3 nN was better than the contrast obtained at 0.1 nN. At least two completely independent experiments were done for each substance, usually many more. In order to minimize drift, the whole setup was allowed to equilibrate for 3−5 h. Drift was further reduced by imaging with relatively high scan frequencies: One image of 512 lines was taken in 8 or 16 s (20−30 Hz). Height, deflection, and friction were used to obtain image contrast. Images shown in this paper were flattened but not further manipulated.

Data Evaluation. The images of the two-dimensional crystals were analyzed to determine the lattice type and the lattice constants. Details of the image analysis are described elsewhere.[28] Before each analysis the images of the two-dimensional crystals were flattened. Then the two-dimensional fast Fourier transformation (2DFFT) was calculated. The positions of the inner spots were noted. To correct for drift, the corresponding spots of two subsequent up and down scans were averaged. All spots were then recalibrated by multiplying them with the appropriate calibration factors for the x- and y-directions. The calibration factors were determined by imaging the hexagonal lattice of mica in air before or after each experiment. The calibration factors were calculated by comparing the measured lattice constant of mica with the known lattice constant of 5.19 Å.[39]

In order to determine the lattice type of the SAMs, all 2DFFTs of one substance were aligned. Thereafter, each 2DFFT was

(27) Wolf, H.; Ringsdorf, H.; Delamarche, E.; Takami, T.; Kang, H.; Michel, B.; Gerber, C.; Jaschke, M.; Butt, H.-J.; Bamberg, E. *J. Phys. Chem.* **1995**, *99*, 7102.

(28) Jaschke, M.; Schönherr, H.; Wolf, H.; Butt, H.-J.; Bamberg, E.; Besocke M. K.; Ringsdorf, H. *J. Phys. Chem.* **1996**, *100*, 2290.

(29) (a) Schönherr, H.; Ringsdorf, H.; Jaschke, M.; Butt, H.-J.; Bamberg, E.; Allison, H.; Evans, S. D. *Langmuir* **1996**, *12*, 3898. (b) Schönherr, H.; Vancso, G. J. *Langmuir* **1997**, *13*, 3769.

(30) (a) Willner, I.; Blonder, R.; Dagan, A. *J. Am. Chem. Soc.* **1994**, *116*, 9365. (b) Spinke, J.; Liley, M.; Schmitt, F.-J.; Guder, H.-J.; Angermaier, L.; Knoll, W. *J. Chem. Phys.* **1993**, *99*, 7012. (c) Weisser, M.; Nelles, G.; Wenz, G.; Mittler-Neher, S. *Sens. Actuators, B* **1997**, *38/39*, 58.

(31) (a) Wilbur, J. L.; Kim, E.; Xia, Y.; Whitesides, G. M. *Adv. Mater.* **1995**, *7*, 649. (b) Tarlov, M. J.; Burgess, D. R. F., Jr.; Gillen, G. *J. Am. Chem. Soc.* **1993**, *115*, 5305. (c) Gorman, C. B.; Biebuyck, H. A.; Whitesides, G. M. *Chem. Mater.* **1995**, *7*, 526.

(32) Gardner, T. J.; Frisbie, C. D.; and Wrighton, M. S. *J. Am. Chem. Soc.* **1995**, *117*, 6927.

(33) Batchelder, D. N.; Evans, S. D.; Freeman, T. L.; Häussling, L.; Ringsdorf, H.; Wolf, H. *J. Am. Chem. Soc.* **1994**, *116*, 1050.

(34) Schaub, M.; Wrighton, M. S. Manuscript in preparation

(35) Nelles, G.; Schönherr, H.; Vansco, G. J.; Butt, H.-J. *Appl. Phys. A: Solids Surf.*, in press.

(36) Wolf, H. Ph.D. Thesis, University of Mainz, 1995.

(37) Callaway, M.; Tildesley, D. J.; Quirke, N. *Langmuir* **1994**, *10*, 3350.

(38) Tupper, K. J.; Colton, R. J.; Brenner, D. W. *Langmuir* **1994**, *10*, 2041.

(39) Güven, N. *Z. Kristallog.* **1971**, *134*, 196.

Table 1. Lattice Types, the Lattice Angles and the Lattice Constants Obtained on SAMs of Different Thiols and Disulfides[a]

		lattice type	angle, deg	lattice constants, Å
diethylalkanoate disulfide	$n = 16$	hexagnoal	60	$a_p = b_p = 5.23$
	$n = 15$	hexagonal	60	$a_p = b_p = 5.29$
	$n = 12$	hexagonal	60	$a_p = b_p = 5.34$
	$n = 10$	hexagonal	60	$a_p = b_p = 5.30$
		centered rectangle	75.7	$a_p = 5.15 \approx b_p = 5.17$
	$n = 8$	hexagonal	60	$a_p = b_p = 5.21$
		oblique	71.0	$a_p = 4.71$, $b_p = 5.47$
diacethylene disulfide		hexagonal	60	$a_p = b_p = 5.40$
ω-hydroxyalkanethiol	$n = 11$	hexagonal	60	$a_p = b_p = 5.33$
ω-carboxyalkanethiol	$n = 15$	oblique	73.3	$a_p = 5.09$, $b_p = 5.33$
anthracenethiol		centered rectangle	75.3	$a_p = 5.31 \approx b_p = 5.30$
anthracene disulfide		centered rectangle	75.9	$a_p = 5.26 \approx b_p = 5.28$
cyclodim. anthracene disulfide		centered rectangle	70.2	$a_p = 5.37 \approx b_p = 5.43$

[a] Values for the primitive unit cells are given.

rotated until it best fitted the 2DFFT of the first image. The mean 2DFFT was calculated by considering all the images, and the alignment was repeated. The lattice parameters were calculated from the measured distances, d_a, d_b, and, for hexagonal lattices, d_c. The distances are related by the following equations to the lattice constants a_p and b_p of the smallest possible unit cell (primitive unit cell) and the angle γ:

$$a_p = d_b/\sin\gamma \quad b_p = d_a/\sin\gamma \tag{1}$$

When hexagonal lattices were obtained, the lattice constant was calculated from

$$a_p = \frac{d_a + d_b + d_c}{3\times \sin 60°} \tag{2}$$

The error for the lattice constants is about 0.1 Å.[28] It is mainly determined by the uncertainty of the scanner calibration. For the angle the error depends on the symmetry of the lattice. For highly symmetric hexagonal lattices it is 2−3° since the aligning procedure tends to enhance random deviations from the 60° angle. Hence, we would not be able to discriminate between a lattice angle of 62 and 60°. For more asymmetric lattices, where the alignment is unambiguous, the error of the angle is about 1° (for details see ref 28).

Results

On large-scale AFM images (500 nm × 500 nm) of SAM covered gold(111) surfaces, islands of roughly 10 Å height separated by flatter regions can be seen. Typically, the islands extended over 30−70 nm. The extensions of the islands and the distances between them differed slightly in different experiments, but no trend could be detected for SAMs of different thiols and disulfides. Figure 2 shows an image of bis[2-(octadecanoyloxy)ethyl] disulfide (n = 16) as an example. High-resolution images of the lattice structures on the islands of SAMs could be obtained. No recognizable periodic structure could be resolved in the flatter regions. It is possible that, between the domains, the molecules are lying flat on the gold substrate. This has been observed for vapor deposited thiols before.[40,41] On the islands two distinctly different types of crystalline structures were observed: Either a hexagonal or a centered rectangular lattice (the only exception is bis[2-(decanoyloxy)ethyl] disulfide (n = 8)). For bis[2-(dodecanoyloxy)ethyl] disulfide (n = 10), a symmetrical disulfide with short alkyl chains, both structural phases were observed: Domains with a hexagonal lattice existed

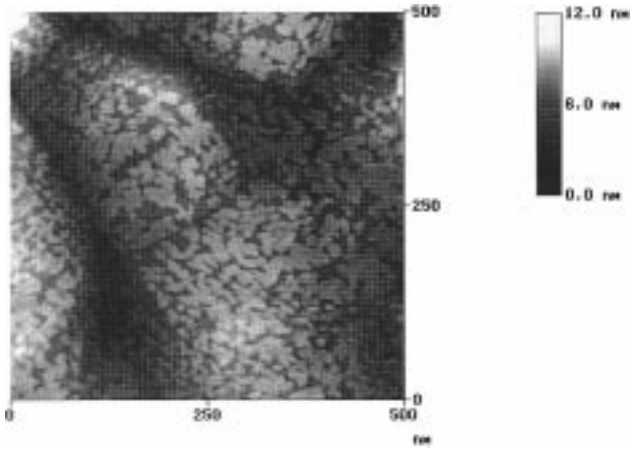

Figure 2. AFM image of bis[2-(octadecanoyloxy)ethyl] disulfides (n = 16) on a gold(111) surface imaged in height mode in ethanol. Elevated crystalline domains are separated by flat disordered regions.

simultaneously with centered rectangular domains. We never observed different lattice structures in a single domain.

Symmetrical diethylalkanoate disulfides $[H_3C(CH_2)_n\text{-}COO(CH_2)_2S]_2$ with long alkyl chains (n = 12, 15, 16) formed SAMs where only lattices with hexagonal structures were observed. Reflections in the 2DFFTs were relatively sharp, indicating that only one distinct lattice was formed (Figure 3). All lattice angles measured centered around a mean angle of 60°, and only a single lattice dimension was observed. The dimensions $d_a \approx d_b \approx d_c$ had average values of 4.53 (n = 16), 4.58 (n = 15), and 4.62 Å (n = 12), leading to lattice constants of 5.23, 5.29, and 5.34 Å, respectively (Table 1). From this the area per thiolate can be calculated to be 23.0, 24.2, and 24.6 Å^2, respectively.

When the chain length was reduced to n = 10, domains with different structures were observed on one sample in the same experiment. That in fact two lattices were formed can be seen in the histograms (Figure 3). Two different angles occurred: one around 60° and one around 76°. Furthermore the distances are widespread, and the histogram contains two peaks. This is a clear indication that one lattice is not sufficient to describe all observed structures. Two lattices are necessary and sufficient to describe the results. One lattice showed a hexagonal structure with a lattice constant of 5.30 Å and an area per thiolate of 24.3 Å^2. The primitive unit cell of the second lattice could be characterized by an angle of 75.7° and lattice constants of a_P = 5.15 Å and b_P = 5.17 Å. Since the two lattice constants are almost identical, the lattice

(40) Himmel, H. J.; Wöll, C.; Gerlach, R.; Polanski, G.; Rubhahn, H. G. *Langmuir* **1997**, *13*, 602.
(41) Poirier, G. E.; Pylant, E. D. *Science* **1996**, *272*, 1145.

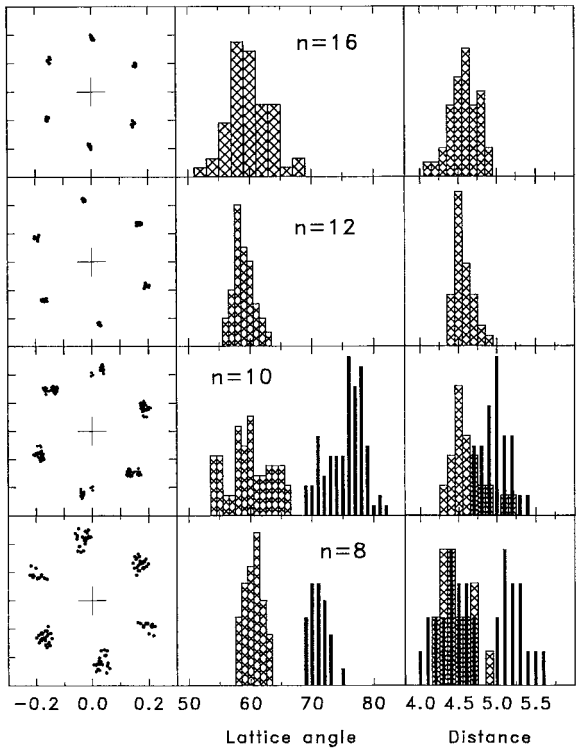

Figure 3. Aligned 2DFFT plots of the crystalline structure of SAMs of the symmetrical diethylalkanoate disulfides $[H_3C-(CH_2)_nCOO(CH_2)_2S]_2$ (n = 8, 10, 12, 16) [the values reported here slightly deviate from earlier values[28] due to a larger number of experiments]. The frequency is also plotted with which a certain angle or a certain distance (Å) was observed (the distances d_a and d_b used in the text and listed in the table should not be mixed up with lattice constants a_p and b_p; to obtain the lattice constants, the distances have to be divided by the sine of the angle according to eq 1). For n = 10 and n = 8 the filled bars in the histograms correspond to the primitive unit cell of the centered rectangular and oblique lattice, respectively, while the cross-hatched bars represent the hexagonal lattices.

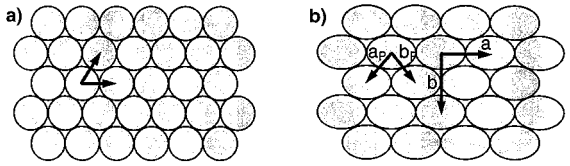

Figure 4. Schematic top view of the densest packing of molecules with (a) a spherical cross-section and (b) a more asymmetrical ellipsoidal cross-section on a surface. The lattice vectors for the primitive unit cell, a_P and b_P, and the centered rectangular unit cell, a and b, are indicated in (b).

can be described with the next higher unit cell as a centred rectangular lattice (see Figure 4) with lattice constants of $a = [5.15^2 + 5.17^2 - 2(5.15)(5.17)\cos 75.7°]^{1/2} = 6.35$ Å and $b = [5.15^2 + 5.17^2 - 2(5.15)(5.17)\cos(180° - 75.5°)]^{1/2} = 8.15$ Å. Such a centered rectangular unit cell contains two thiolates. The area per thiolate is 25.8 Å^2. A comparison of the two different lattices is shown in Figure 5.

When the chain length was further reduced to n = 8, about 40% of the domains still showed lattices with a hexagonal structure and a lattice constant of 5.21 Å. Most of the other domains could be described by an oblique lattice with an angle of 71.0° and lattice constants of a_p = 4.71 Å and b_p = 5.47 Å. This leads to an area per thiolate of 24.2 Å^2. With bis[2-(octanoyloxy)ethyl] disulfide (n = 6) no two-dimensional crystalline structure was observed

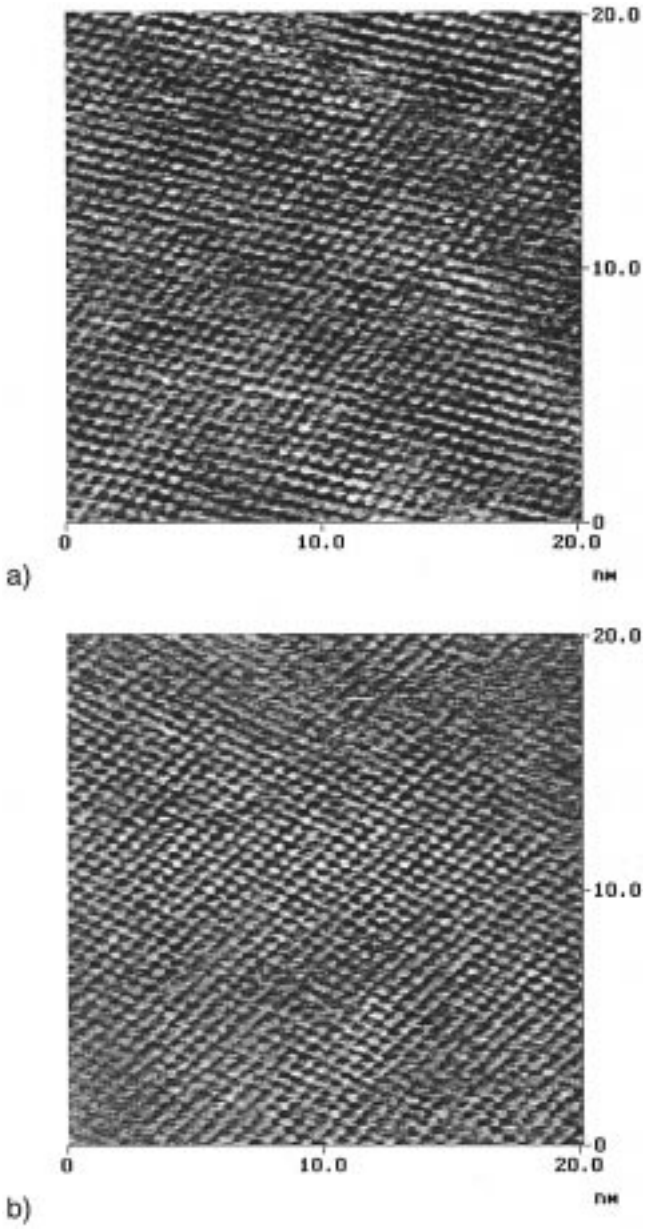

Figure 5. Comparison of crystalline domains in a SAM of bis-[2-(dodecanoyloxy)ethyl] disulfides (n = 10) on a gold(111) surface imaged with an AFM in friction mode in ethanol. (a) A domain with a hexagonal structure is shown. (b) The image shows a centered rectangular lattice. Both images were obtained in the same experiment on the same sample.

anymore. We cannot decide whether really no crystalline domains existed or if they just could not be imaged with the AFM.

The quantitative analysis of lattice structures formed by the asymmetrical diethylalkanoate disulfides (m = 16, n = 11...15) showed crystalline domains similar to the SAMs of the symmetrical long-chain diethylalkanoate disulfides. They can be described as hexagonal despite there being a chain length difference of five methylene units between neighboring chains (n = 11) (Figure 6b). The lattice angles are around 60° with lattice constants of 5.32 (n = 15), 5.23 (n = 14), 5.24 (n = 13), 5.18 Å (n = 12), and 5.32 Å (n = 11), respectively. Though the lattice constants did not change significantly, the observed contrast decreased with increasing asymmetry. In all cases, the best contrast was obtained at roughly the same force (1−2 nN). The area per thiolate can be calculated to be 24.5, 23.7, 23.8, 23.2, and 24.5 Å^2, respectively. These

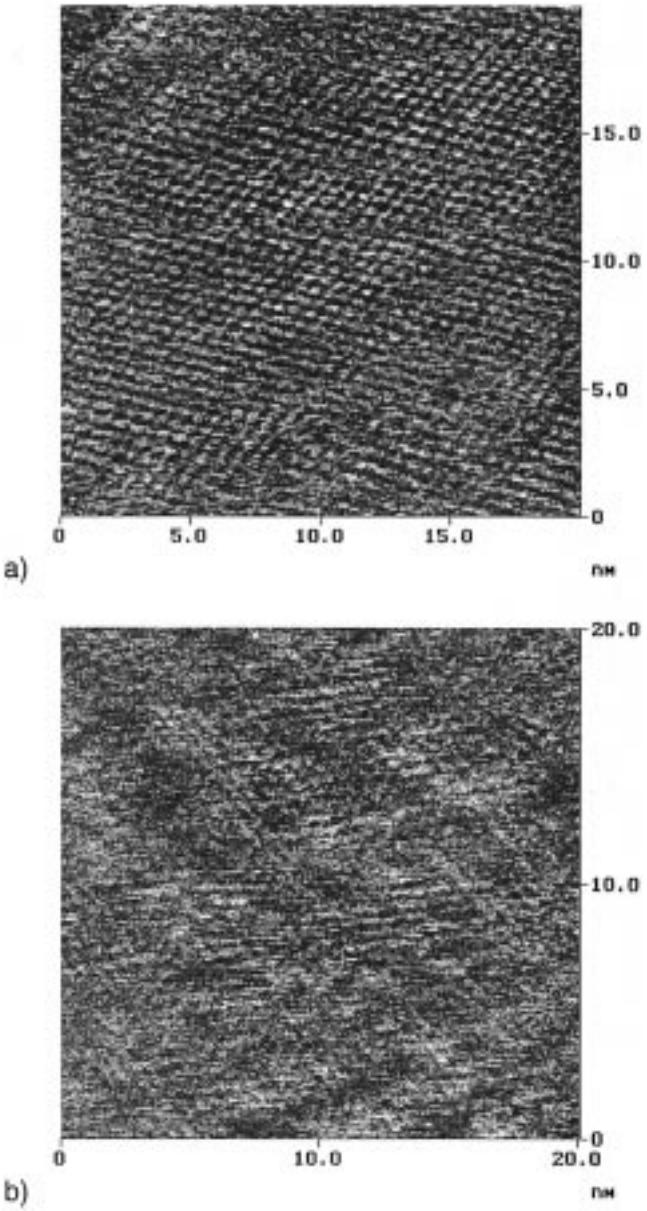

Figure 6. Comparison of crystalline domains in SAMs of (a) bis[2-(octadecanoyloxy)ethyl] disulfide ($n = 16$) and of (b) the asymmetrical 2-(octadecanoyloxy)-2′-(tridecanoyloxy)-1,1′-diethyl disulfide ($m = 16$, $n = 11$) on gold(111) surfaces imaged with an AFM in friction mode in ethanol.

values are in good agreement with parameters obtained on SAMs of symmetrical disulfides.

In addition to the quantitative analysis of the lattices formed by the disulfides, the orientation of the adsorbate lattice with respect to the underlying gold(111) lattice was analyzed. On bare gold(111), single monocrystalline terraces extending up to several nanometers could be found. In some cases triangular terraces were observed. These were aligned on areas of up to 2 μm. The preferred orientation of the gold(111) lattice is determined by the mica substrate.[42] The edges of triangular terraces represent nearest neighbor directions of the gold atoms in the lattice. By determination of the orientation of the adsorbate lattice on such a triangular terrace, we were able to determine the orientation of SAMs with respect

(42) (a) Reichelt, K.; Lutz, H. O. *J. Cryst. Growth*. **1971**, *10*, 103. (b) Chidsey, C. E. D.; Loiacoho, D. N.; Sleator, T.; Nakahara, S. *Surf. Sci.* **1988**, *200*, 45.

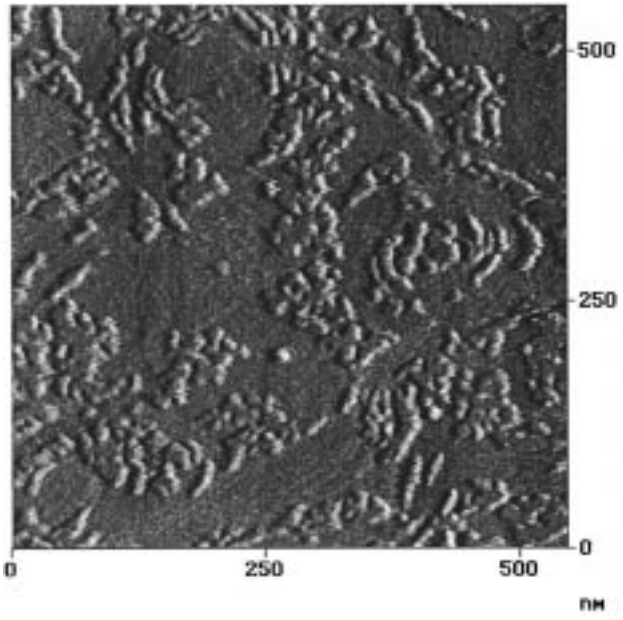

Figure 7. AFM image of the asymmetrical 2-(octadecanoyloxy)-2′-(tetradecanoyloxy)-1,1′-diethyl disulfide ($m = 16$, $n = 12$) adsorbed on gold(111) substrate taken in ethanol in deflection mode. Elevated crystalline domains are separated by flat disordered regions. In addition, equilateral triangular terraces determined by the underlying gold(111) can be seen.

to the underlying gold(111). For example, the lattice of the SAM of the asymmetric diethylalkanoate ($m = 16$, $n = 12$) was found to be rotated by $30 \pm 2°$ with respect to the edges of the terraces and thus the underlying gold(111) lattice (Figure 7).

Diacetylene disulfides formed hexagonal lattices on gold(111) surfaces with a lattice constant of 5.40 Å. This leads to an area per thiolate of 25.3 Å^2. Though the images had a high contrast, the lattice angles were relatively widely distributed (Figure 8). Hydroxy terminated thiols on gold(111) surfaces are also adsorbed in domains with hexagonal structures. The analysis of the 2DFFT leads to a lattice angle of 60° and a lattice constant of 5.33 Å, corresponding to an area of 24.6 Å^2. The lattice constant is close to the constants of long-chain diethylalkanoate disulfides ($n \geq 12$).

In contrast, SAMs of carboxy terminated thiols showed an oblique lattice structure similar to that of the short-chain diethylalkanoate disulfide ($n = 8$). This hints that the position of the carboxy group within the layer influences the lattice structure formed through adsorption on gold surfaces. The lattice angle of the carboxy terminated layers is 73.3°, and the lattice constants were found to be 5.09 and 5.33 Å, resulting in an area of 26 Å^2 per thiolate. It was not possible to obtain a good contrast on carboxy terminated thiols by measuring in ethanol. Therefore it was necessary to image in water containing 1 mM $CaCl_2$. Even then, the contrast was not as good as on SAMs of the symmetrical disulfides imaged in ethanol (Figure 9).

Anthracene terminated thiols and disulfides with the anthracene anchored at the 2 position formed centered rectangular lattices. This can be deduced from the fact that the lattice constants of the primitive unit cell were indistinguishable ($a_p = 5.31$ Å $\approx b_p = 5.30$ Å; see Table 1). The lattice constants of the centered rectangular lattice were 6.48 and 8.40 Å for anthracenethiols and 6.48 and 8.31 Å for anthracene disulfide. Hence, within the error of our measurements, thiols and dislufides formed the same lattices. The area per thiolate was 27.1 Å^2. We

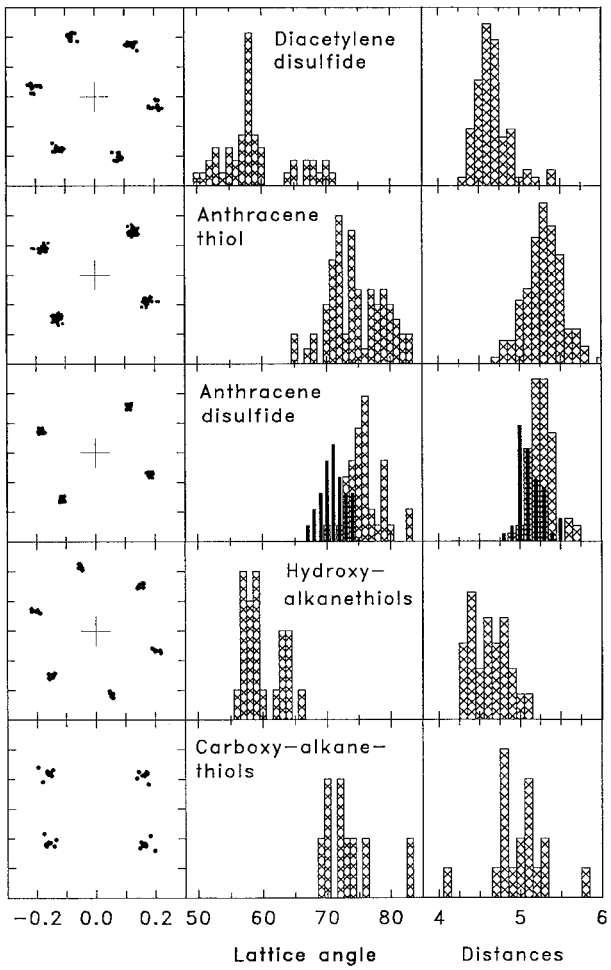

Figure 8. Aligned 2DFFT plots of the crystalline structure of SAMs of diacetylene disulfide, anthracene terminated thiols and disulfides, and hydroxy and carboxy terminated thiols. In addition, the frequency is shown with which a certain angle or a certain distance was observed (the distances d_a and d_b used in the text and listed in the table should not be mixed up with lattice constants a_p and b_p; to obtain the lattice constants, the distances have to be divided by the sine of the angle according to eq 1). For anthracene disulfide filled bars in the histograms correspond to the values of the photocyclodimerized derivative, while the cross-hatched bars represent the open derivative.

could not resolve clear periodic structures of SAMs on gold(111) when we used thiols which comprised derivatives where the anthracene was bound at the 9 position.

Acetylenes[33] and anthracenes[34] are known to cross-link through exposure to light. After illuminating SAMs of anthracene disulfides with a certain wavelength which induces the [4 + 4]-photocyclodimerization in solution (360 nm), we were, however, unable to detect any difference in the lattice parameters compared to the initial values. As a control experiment, we did the photocyclodimerization of anthracene disulfides in solution before adsorption on gold. Then we imaged the SAM in ethanol. The lattice angle of the primitive unit cell of cyclodimerized SAMs was reduced to 70.2° (see Table 1 and Figure 8). After imaging, we illuminated the layer at 250 nm to cleave the cyclodimerization product and imaged the layer again. The analysis of the lattices gave similar values for lattice angles and constants of both measurements: 70.2°, 5.43 Å, and 5.37 Å without cleavage and 71°, 5.56 Å, and 5.37 Å after cleaving with UV light of 250 nm wavelength. Hence, the two-dimensional packing of SAMs seems to be determined by the structure of the disulfides during adsorption. In contrast to our experiments, Schaub and

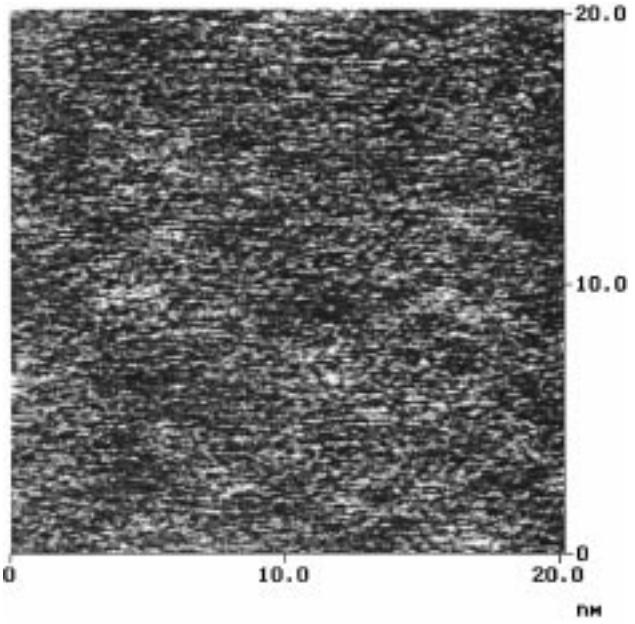

Figure 9. Crystalline domain in SAMs of carboxy terminated thiols on gold(111) surfaces imaged with an AFM in friction mode in water with 1 mmol of $CaCl_2$. Because of the carboxy group, the obtained contrast is poor.

Wrighton[34] were able to detect the cleavage of the cyclodimerization product of anthracene disulfide by using cyclic voltammetry and fluorescence spectroscopy measurements. However, they were also unable to detect the photocyclodimerization within the SAMs.

Discussion

When the two-dimensional structures of SAMs of thiols and disulfides on gold(111) which have been studied so far (Table 2) are reviewed, two general observations emerge. First, up to now, no significant difference was observed between the two-dimensional structures of thiols and disulfides. This agrees with a conclusion reached by others.[43,44] Second, SAMs of small thiols and disulfides formed crystalline domains with either hexagonal or distinctly different centered rectangular structures (the only exception is bis[2-(decanoyloxy)ethyl] disulfide). The angles of the primitive unit cells observed are either 60° or 76−78°, which indicates that really two classes of lattices are formed. No lattices with angles between 63 and 75° could be detected. Even when the chain length of the diethylalkanoate disulfides was reduced, no gradual change occurred.

With the symmetrical diethylalkanoate disulfides adsorbed on gold(111), surfaces of both kinds of lattices mentioned were detected. Such a coexistence of two crystalline phases was observed earlier with azobenzenethiols and disulfides on gold.[28] In contrast to the earlier results, in this case we could identify the factor which determines the formation of two different crystalline phases: The length of the alkyl chains is the decisive factor. A centered rectangular or oblique structure is assumed by disulfides with short alkyl chains (n = 10 or 8, respectively). They are dominated by the relatively asymmetric ester groups which show a kind of elliptical cross-section (for disulfide the shape of the thiolates is considered). With increasing chain length the hexagonal

(43) Bain, C. D.; Biebuyck, H. A.; Whitesides, G. M. *Langmuir* **1989**, *5*, 723.
(44) Biebuyck, H. A.; Bain, C. D.; Whitesides, G. M. *Langmuir* **1994**, *10*, 1825.

Table 2. Two-Dimensional Structures of Thiols and Disulfides Adsorbed on Gold Surfaces Known to the Authors[a]

class	substance	lattice type	lattice angle deg	lattice constant, Å	ref	method
A	$H_3C(CH_2)_nSH$	hexagonal	60	5.0	12, 18, 19, 21, 22, 51, 24	LEED He diff,
	$H_3C(CH_2)_nSS(CH_2)_nCH_3$ n = 9, 11, 13, 17, 21				62, 53, 54, 55, 56	AFM, STM
	$[H_3C(CH_2)_nCOO(CH_2)_2S]_2$ n = 12, 15, 16	hexagonal	60	5.3	28, this work	AFM
	$[H_3C(CH_2)_{10}COO(CH_2)_2S]_2$	hexagonal	60	5.3	28, this work	AFM
		centered rectangle	76	5.2		
	$[H_3C(CH_2)_8COO(CH_2)_2S]_2$	hexagonal	60	5.2	this work	AFM
		oblique	71	4.7, 5.5		
	$[H_3C(CH_2)_{13}C{\equiv}CC{\equiv}C(CH_2)_9COO(CH_2)_2S]_2$	hexagonal	60	5.4	this work	AFM
	$H_3C(CH_2)_{16}SS(CH_2)_nCH_3$ n = 11−15	hexagonal	60	5.2−5.3	this work, 35	AFM
B	$HO(CH_2)_{11}SH$	hexagonal	60	5.33	this work, 57	AFM
		hexagonal	60	5.0		STM
	$H_3C(CH_2)_{11}SS(CH_2)_{11}OH$	hexagonal	60	5.0	58	STM
C	$HOOC(CH_2)_{15}SH$	oblique	73	5.3, 5.1	this work	AFM
D	$F_3C(CF_2)_n(CH_2)_2SH$ n = 5, 7, 11	hexagonal	60	5.7−5.8	25, 26	AFM
	$[F_3C(CF_2)_7(CH_2)_2COO(CH_2)_2S]_2$	hexagonal	60	5.9	28	AFM
	$F_3C(CF_2)(CH_2)_6SH$	hexagonal	60	5.2	59	AFM
E	$F_3C(CF_2)_n(CH_2)_2COO(CH_2)_2S-$ $S(CH_2)_2OOC(CH_2)_mCH_3$ n = 6, 7, m = 9, 10	hexagonal	60	6.2	28	AFM
F	$(C_6H_5)N{=}N(C_6H_4)O(CH_2)_nSH$	centered rectangle	76	5.0	27, 28	STM
	$[(C_6H_5)N{=}N(C_6H_4)O(CH_2)_nS]_2$ n = 6, 11					AFM
	$H_3CO(C_6H_4)N{=}N(C_6H_4)O(CH_2)_{11}SH$ $[H_3CO(C_6H_4)N{=}N(C_6H_4)O(CH_2)_{11}S]_2$	centered rectangle	78	5.2	28	AFM
G	$(C_{14}H_9)COO(CH_2)_{11}SH$ $[(C_{14}H_9)COO(CH_2)_{11}S]_2$	centered rectangle	76	5.3	this work	AFM

[a] Several classes have been investigated: A, long-chain *n*-alkanethiols and symmetrical and asymmetrical disulfides; B, ω-hydroxyalkane thiols and disulfides; C, ω-carboxyalkane thiols; and D, fluorinated alkanethiols; E, mixed hydrated and fluorinated alkane dislufides; F, ω-azobenzenealkane thiols and disulfides; G, ω-anthracenealkanethiols and disulfides. In addition to the lattice type, angle and constants for the primitive unit cells are reported. The techniques employed are low-energy electron diffraction (LEED), low-energy helium diffraction (He diff), scanning tunnelling microscopy (STM), and AFM.

lattice occurs more frequently, in agreement with the belief that now the more spherical cross-sections of the alkyl chains dominate the elliptical cross-sections of the ester groups. In addition, carboxy terminated alkylthiols formed an oblique lattice structure, whereas SAMs of hydroxy terminated alkanethiols showed a hexagonal structure.

These findings yield a simple empirical rule: Thiols and disulfides with relatively spherical cross-sections (for disulfide the shape of the thiolate is considered), like alkanethiols or hydroxy terminated or fluorinated alkanethiols, tend to form hexagonal lattices. Thiols with more asymmetric cross-sections, like the azobenzenethiols, and the anthracene derivatives crystallize in the form of centered rectangular lattices. The only exceptions were ω-carboxyalkanethiols (however, images of SAMS of carboxy terminated thiols showed a low contrast, and, to obtain a contrast, Ca^{2+} and water were necessary; this is a hint that other factors contribute to the structure, and the mechanisms of getting contrast in water or ethanol are different). A tentative simple explanation for this empirical rule is that thiols tend to pack in the densest way possible. The densest packing for molecules with a spherical cross-section is the hexagonal packing. In contrast, for asymmetric molecules, which as a first approximation have an elliptical cross-section, a centered rectangular structure yields the densest packing (Figure 4). The driving force for dense packing is strong binding to the gold substrate. The high binding energy ensures that as many molecules bind to the gold surfaces as possible. The effect is really similar to a high pressure being applied to a monolayer on a water surface.

This hypothesis explains the formation of hexagonal and centered rectangular lattices and its dependence on shape and symmetry of molecules. It does not explain why only certain centered rectangular lattices occur (those with lattice angles of 76−78° in the primitive unit cell) and no intermediate lattices (with lattice angles between 63−75°). We have as yet no explanation for the occurrence of only distinct lattice angles.

The simple empirical rule concerning the crystalline structure of SAMs on gold is only followed by thiolates with a relatively *small* cross-section. The largest molecules studied were the fluorinated alkanethiols[28,29] and the azobenzenethiols with cross-sectional areas of 25−30 Å^2. Thiols with a larger cross-section, like the anthracene derivative anchored at the 9 position, cyclodextrins,[45] or different discoid molecules,[46] do not form a two-dimensional lattice structure at all.

Furthermore, we would like to point out that most two-dimensional structures listed in Table 2 were revealed by using atomic force microscopy. It is not totally clear how at the atomic scale the contrast in atomic force microscopy images arises. Several arguments show that the contrast does not reflect the structure of the underlying gold or the sulfur atoms but that it is caused by the tail groups (see also refs 28 and 29). Consequently no direct information about the question of whether or not the thiols bind as thiolates or disulfides can be obtained. We would, however, like to point out that for the disulfides studied we can exclude a phase separation of disulfides with different chains at room temperature. If for instance $H_3C(CH_2)_nCOO(CH_2)_2S-S(CH_2)_2OOC(CH_2)_mCH_3$ with m = 16 and n = 11 phase separates after dissociation, we would have observed hexagonal lattices of $H_3C(CH_2)_{16}COO(CH_2)_2$, and centered rectangular lattices formed by $H_3C(CH_2)_{11}COO(CH_2)_2S$. Instead we only observed hexagonal lattices with relatively low contrast.

A phase separation would indicate that disulfides dissociate on the gold surface. Such a phase separation was observed by Ishida *et al.* with asymmetric hydrocarbon-fluorocarbon disulfides.[47] When annealing SAMs at

(45) Nelles, G.; Weisser, M.; Back, R.; Wohlfart, P.; Wenz, G.; Mittler-Neher, S. *J. Am. Chem. Soc.* **1996**, *118*, 5039.

(46) Schöherr, H.; Kremer, F.; Kumar, S.; Rego, J. A.; Wolf, H.; Ringsdorf, H.; Jaschke, M.; Butt, H.-J.; Bamberg, E. *J. Am. Chem. Soc.* **1996**, *118*, 13051.

(47) Ishida, T.; Yamamoto, S.; Mizutani, W.; Motomatsu, M.; Tokumoto, H.; Hokari, H.; Azehara, H.; Fujihira, M. *Langmuir* **1997**, *13*, 3261.

100 °C for 8 h, they observed a phase separation. In contrast, Jaschke *et al.*[28] were unable to observe such a phase separation with asymmetric hydrocarbon−fluorocarbon disulfides, where the alkyl and fluorinated alkyl chains were linked via an ester bond. Ishida *et al.* explained the negative result by speculating that at 100 °C the ester bond is cleaved and the alkyl chains dissociate. This, however, was shown not to happen since Jaschke *et al.* were able to resolve the original crystal lattice formed by the asymmetric molecule at room temperature.

On SAMs of asymmetrical diethylalkane disulfides with chain length differences up to five methylene units, domains with hexagonal lattice structures could be imaged. This demonstrates that the "depth of contrast" or "information depth" lies several angstroms, at least five methylene groups, in the SAMs and confirms that it is not only the end groups that are responsible for the contrast. Taking the five methylene groups as the information depth, one can estimate a value of at least 6 Å. Liu and Salmeron[12] could displace *n*-alkanethiols and image the underlying gold(111) lattice at forces above 280 nN. Hence, at normal imaging conditions, that is, with forces of 1−10 nN, the tip does not completely penetrate the monolayer. On the other hand, to be able to resolve the hexagonal lattice of alkanethiols on gold, Butt *et al.*[24] needed to apply a minimum force of 0.1 nN. Low-energy helium diffraction and FTIR studies have indicated that the thermal motion of the outermost methyl groups at room temperature leads to the formation of terminal gauche defects.[2,21,48] The minimal force of 0.1 nN was probably necessary to penetrate the outermost methyl groups.

As a first approximation one could identify the "information depth" with the "penetration depth" of the tip into the SAM. Having an estimate of the penetration depth z and knowing the applied force, one can calculate the elastic modulus of the thiol monolayer. Since this can only be a rough estimate anyway, we use the Hertz model,[49] thus neglecting surface forces and only taking the elastic behavior of the substrate into account. In the Hertz model the applied force F, the elastic modulus of the substrate E, the Poisson number ν, and the radius of curvature of the tip R are related by

$$z^3 = \frac{9}{16}\left(\frac{1-\nu^2}{E}\right)^2 \frac{F^2}{R} \qquad (3)$$

With $z = 6$ Å, $F = 2$ nN, $R = 5$ nm (as given by the manufacturer), and $\nu = 0.3$ (a reasonable value for most materials) one obtains an elastic modulus of $E = 1.3$ GPa. Since a penetration depth of 6 Å is probably a lower limit for the true value, the estimated elastic modulus is an upper limit. Nevertheless, it agrees with the result obtained by Thomas *et al.*,[11] who estimate a value of 1 GPa, and is also in the range of a result of Kiridena *et al.*, who measured a values of 0.6 GPa.[50]

With Hertz theory one can estimate the contact radius a or the contact areas:

$$a^3 = \frac{3}{4}\frac{1-\nu^3}{E}RF \qquad (4)$$

Using the values above, a contact radius of 1.8 nm results. Hence, under these imaging conditions one could not expect to achieve true atomic resolution, but the images more represent the mean periodicity within an area of roughly 2 nm diameter.

Conclusion

Several classes of thiols and disulfides were adsorbed on gold(111) surfaces. In all cases domains with crystalline structure separated by disordered regions could be observed. By changing the shape of the molecules different types of lattices were observed, leading to a simple empirical rule: Thiols and disulfides (for disulfides the shape of the thiolates is considered) with relatively spherical cross-sections, for example alkanethiols or hydroxy terminated or fluorinated alkanethiols, form hexagonal lattices. Thiols with more asymmetric cross-sections, like carboxy terminated thiols, azobenzenethiols, or anthracene derivatives, crystallize in the form of centered rectangular lattices. To our knowledge up to now, all *small* thiols (or disulfides) seem to fit into this simple empirical rule. The rule indicates that the symmetry of the molecules is one decisive factor for the two-dimensional packing, but the symmetry alone, however, cannot explain the switch between hexagonal and centered rectangular packing in the case of bis[2-(dodecanoyloxy)ethyl] disulfide ($n = 10$), a symmetrical disulfide with short alkyl chains where both structural phases were observed in different domains beside each other. Hence, other factors seem to influence the packing of thiols on gold. Furthermore, asymmetrical diethylalkanoate disulfides, with chain length differences up to five methylene units between neighboring chains, were shown to self-assemble on gold(111) surfaces with the formation of hexagonal lattices. This indicates, that the AFM tip penetrates at least five methylene units into the SAMs.

Acknowledgment. The authors would like to thank Dr. Ram Seshadri for discussions. This work was supported by the Ernst-Rudolf-Schloessmann-Stiftung (G.N.), the Foundation for Chemical Research in the Netherlands (SON, H.S.), the Deutsche Forschungsgemeinschaft (H.S.), especially by the Schwerpunktprogramm *Neue mikroskopische Techniken für Biologie und Medizin* (M.J., H.-J.B.), and a NATO-Science fellowship of the German Academic Exchange Service DAAD (M.S.).

LA9709709

(48) Nuzzo, R. G.; Korenic, E. M.; Dubois, L. H. *J. Chem. Phys.* **1990**, *93*, 767.
(49) (a) Hertz, H. *J. Reine Angew. Math.* **1881**, *92*, 156. (b) Landau, L. D.; Lifshitz, E. M. *Lehrbuch der Theoretischen Physik VII*; Akademie-Verlag: Berlin, 1965. (c) Timoshenko, S. P.; Goodier, J. N. *Theory of Elasticity*; McGraw-Hill: New York, 1970.
(50) Kiridena, W.; Jain, V.; Kuo, P. K.; Liu, G. *Surf. Interface Anal.* **1997**, *25*, 383.
(51) Camillone, N.; Chidsey, C. E. D.; Liu, G. Y.; Scoles, G. *J. Chem. Phys.* **1993**, *98*, 4234.
(52) Pan, J.; Tao, N.; Lindsay, S. M. *Langmuir* **1993**, *9*, 1556.
(53) Delamarche, E.; Michel, B.; Gerber, C.; Anselmitti, D.; Güntherodt, H. J.; Wolf, H.; Ringsdorf, H. *Langmuir* **1994**, *10*, 2869.
(54) Poirier, G. E.; Tarlov, M. J. *Langmuir* **1994**, *10*, 2853.
(55) Rolandi, R.; Cavalleri, O.; Toneatto, C.; Ricci, D. *Thin Solid Films* **1994**, *243*, 431.
(56) Schönenberger, C.; Jorritsma, J.; Sondag-Huethorst, J. A. M.; Fokkink, L. G. J. *J. Phys. Chem.* **1995**, *99*, 3259.
(57) Sprik, M.; Delamarche, E.; Michel, B.; Röthlisberger, U.; Klein, M. L.; Wolf, H.; Ringsdorf, H. *Langmuir* **1994**, *10*, 4116.
(58) Takami, T.; Delamarche, E.; Michel, B.; Gerber, C.; Wolf, H.; Ringsdorf, H. *Langmuir* **1995**, *11*, 3876.
(59) Motomatsu, M.; Mizutani, W.; Nie, H. Y.; Tokumoto, H. *Thin Solid Films* **1996**, *281−282*, 548.